

USING INFRARED BASED RELATIVE NAVIGATION FOR ACTIVE DEBRIS REMOVAL

Özgün Yılmaz⁽¹⁾, Nabil Aouf⁽¹⁾, Laurent Majewski⁽²⁾, Manuel Sanchez-Gestido⁽³⁾, Guillermo Ortega⁽³⁾

⁽¹⁾ *Cranfield University, Shrivenham United Kingdom, {o.yilmaz,n.aouf}@cranfield.ac.uk*

⁽²⁾ *SODERN, Limeil-Brevannes France, Email: laurent.majewski@sodern.fr*

⁽³⁾ *European Space Agency, Noordwijk The Netherlands, Email: manuel.sanchez.gestido@esa.int*

ABSTRACT

A debris-free space environment is becoming a necessity for current and future missions and activities planned in the coming years. The only means of sustaining the orbital environment at a safe level for strategic orbits (in particular Sun Synchronous Orbits, SSO) in the long term is by carrying out Active Debris Removal (ADR) at the rate of a few removals per year.

Infrared (IR) technology has been used for a long time in Earth Observations but its use for navigation and guidance has not been subject of research and technology development so far in Europe. The ATV-5 LIRIS experiment in 2014 carrying a Commercial-of-The-Shelf (COTS) infrared sensor was a first step in de-risking the use of IR technology for objects detection in space. In this context, Cranfield University, SODERN and ESA are collaborating on a research to investigate the potential of IR-based relative navigation for debris removal systems. This paper reports the findings and developments in this field till date and the contributions from the three partners in this research.

1 INTRODUCTION

The precise relative navigation of a chaser spacecraft towards a dead satellite is one of the most difficult tasks to accomplish within an ADR mission, due to the fact that target is uncooperative and in general in an unknown state [1]. The current Guidance Navigation & Control (GNC) systems technology can handle cooperative rendezvous, but for an ADR mission the number of unknowns is greater than an ordinary mission and further developments are needed [2].

Since there are more uncertainties in the navigation function of an ADR mission, it is favourable to have continuous measurements which would require sensors working in all environmental conditions possible [3]. The vision-based cameras, which are already suffering from poor illumination conditions even in cooperative rendezvous with 3-axis stabilized target holding fiducial markers, cannot match the IR cameras that can perform in all possible illumination conditions of ADR. An infrared camera can overcome the illumination problem by providing information without any discontinuity as it does not depend on external light source but the emitted radiation.



Figure 1: Infrared image of International Space Station from LIRIS experiment (courtesy of SODERN) [5]

Long wave infrared (LWIR) imaging techniques offer many potential benefits when applied to the remote sensing of space debris. Imaging space objects in the LWIR band has the inherent advantage of not being dependent upon constant Solar or Earth illumination which makes the observations and measurements possible even when observed objects are in eclipse. This fact had been confirmed by ATV-5 LIRIS experiment data [4][5] in which International Space Station (ISS) could be observed in any illumination conditions (Figure 1).

The appearance of objects under Sun direct illumination is expected to be smoother in infrared when compared to the reflection of visible light on reflecting surfaces like multi-layer insulation. Imaging space objects in the LWIR band may also allow for the imaging of objects looking at with the Sun in the field of view without saturation of the imaging system and also without permanent damage. So challenges in terms of illumination changes could be dealt with using an infrared-based rendezvous sensor providing navigation data for flexible relative navigation and guidance to targets.

2 ACTIVE DEBRIS REMOVAL CONCEPT

The Active Debris Removal missions can be considered as a variant of Rendezvous and Docking (RvD) missions where the target is uncooperative meaning that there are no fiducial markers on target and relative orientation of target cannot be known [6]. Furthermore, the targets would be most likely old satellites where available geometrical model may not fit to actual orbiting body due to changes in its configuration at time of its launch or target may have experienced a collision which changed its geometry. In broad context, such mission would consist of seven phases: rendezvous, inspection, fly-around, final approach, capture, stabilisation and de-orbiting ([7]). A representative mission profile up to capture had been depicted in Figure2 however reader shall be aware that it is just for visualisation purposes in order to ease the text and an actual mission could have a slightly different trajectory depending on target attributes.

In the rendezvous phase, chaser spacecraft transfers to target orbit and phases with the target object. In the beginning of this phase, the chaser spacecraft would use the absolute navigation system which would be handed over to a relative navigation system towards the end. Considering the uncooperative

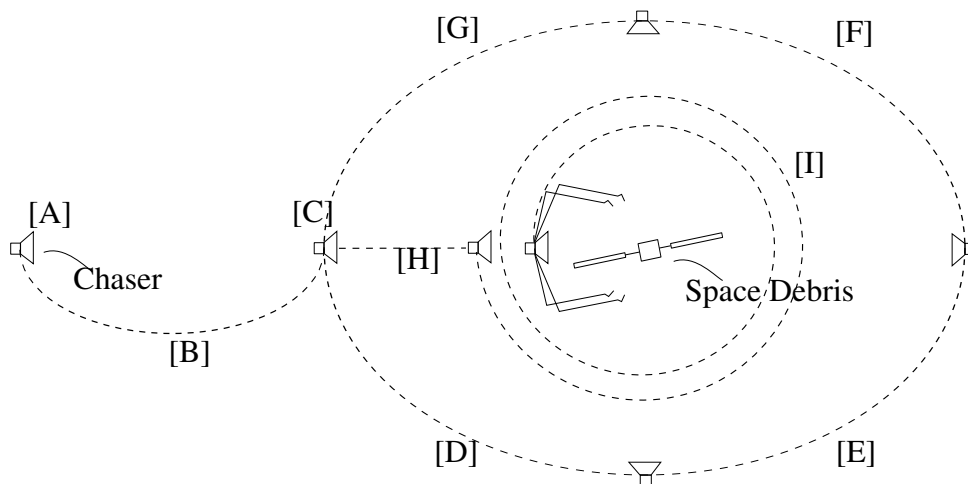


Figure 2: Graphical representation of Active Debris Removal at close proximity operations

nature of the target, the chaser would only be able to use active sensors like LIDAR which has more limitations on target range or passive sensors like camera [8] in the relative navigation part. At the end of this, the chaser would be at holding point-[A] (Figure2).

In the inspection phase, the chaser could observe space debris for the required amount of time to gather enough information to enable the planning of the further steps of the ADR. At this stage, navigation algorithm is expected to provide relative position and velocity of the chaser in target Local Vertical Local Horizontal (LVLH) frame and could benefit from infrared based techniques. This phase could involve some sort of approach like depicted as phase-[B] (Figure2) to allow better inspection if the navigation solution require such.

The fly around phase is to verify the information gathered in the inspection phase. It is most likely to happen in the same orbital plane in order to keep fuel consumption at minimum. The fly-around phase is used to determine the attitude rate of the target and match it [9][10][11]. This phase is needed to identify the best possible place to initiate the capture and could benefit from infrared based techniques to accurately and autonomously determine the best capture pose. In order to do so, the chaser could stay in a hold point-[C] at the end of fly around phase if the navigation algorithm required to do so.

The final approach and capture depends on the estimated motion of the target as the chaser needs to be aligned with the target. Even though the accuracy of the alignment depends on the target attitude, this part is one of the most challenging part of the mission for the cases where the target tumbles and the

measurement updates play a crucial role for Guidance, Navigation and Control (GNC) perspective. In Figure 2, this phase is depicted as phase-[H] and phase-[I]. In this sample trajectory, the target is tumbling around H-bar of LVLH frame and therefore approach could be in plane. However, such conditions would be the best case of ADR for final approach and also the least likely to happen in reality.

In the stabilisation and de-orbiting case, the chaser aims to damp the tumbling motion of the target in order to control the target to de-orbit by provided de-orbiting mechanism (e.g. solar sailing, electric tether) of the ADR mission.

3 CHASER NAVIGATION

The proposed chaser sensing suite used in this research activity has been classified into long range, medium range, and close range sensors. For an ADR mission, the ESA proposed sensing suite selected is composed of two star trackers (STR), two Inertial Measurement Units (IMU), two infrared cameras (IRCAM), two Light Detection And Ranging (LIDAR) units, and one Global Positioning Service (GPS) receiver. Except the GPS which can only provide information about absolute positioning, all other equipments are provided with their redundancy for the safety of the mission. Therefore, navigation algorithms shall be designed only for single equipment meaning that stereo vision would not be applicable for the study. Sun acquisition is obtained by the mounting of Digital Sun Sensors (DSS).

The algorithms can be embedded in smart sensors providing the navigation data expected from their sensing. This is already the case for star trackers and smart cameras embedding image processing up to 6 DoF pose measurement are expected in near future.

The IMU and the STR would provide classic absolute navigation as well as redundancy for the phasing part of the rendezvous and the fly around part. These sensors will also provide a navigation solution during the capture and during the de-orbiting part. The objective of the GPS receiver is to measure the absolute position during phasing and shall act as long-range sensor. The LIDAR provides the measurements of the relative distance with the target at close range. On the other hand, infrared and visual cameras support the navigation solution from rendezvous until the capture phase.

The infrared sensor used in this research is similar to the ones flown on the ESA-Airbus-SODERN-JenaOptronik experiment called LIRIS [4]. LIRIS was a test of European sensors technology in space to improve the autonomous rendezvous and docking that ATVs have performed five times since 2008 for future noncooperative rendezvous. The experiment had one LIDAR provided by JenaOptronik from Germany, one visual camera and two infrared cameras provided by SODERN from France.

4 TARGET ILLUMINATION

Target illumination is an important constraint for visual navigation in space applications. There are two different cases where visual navigation systems fails: certain chaser-target-sun geometries and

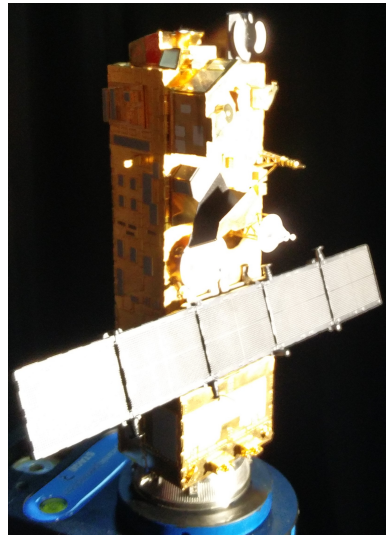


Figure 3: Unfavourable illumination condition effects in visual camera

eclipse/shadowing. Some space surface coatings have specular reflection properties, combining with direct solar illumination they can saturate the visual detectors depending on the chaser-target-sun geometry such as one envisaged in Figure3. This unavoidable case causes problems for visual navigation which looks for visual cues.

In the study of [12] which is a navigation algorithm for partially cooperative targets, it had been shown that the accuracy varies by three folds in close range depending on the target illumination condition and was suggested to be more for farther targets. In the case of eclipse/shadowing, target is either partially or fully not observable therefore there is not enough visual cues to be used in navigation filter. Shadowing can be due to the geometry of the target by self obstruction or in close range to chaser's shadow on the target due to chaser-target-sun geometry. For certain cases, this lack of measurement can be somehow tolerated depending on its duration. However, the navigation filter would be less tolerant to the uncertainties in the modelling of the orbital dynamics. Considering the dynamics of relative navigation, such confidence in process model is not actually viable to rely on it.

Unfortunately, the target illumination conditions of an ADR scenario are more challenging than an ordinary cooperative rendezvous mission because avoiding such geometries by mission planning cannot be enforced for various reasons. There are more uncertainties in the system as the target is uncooperative and our knowledge about the target is limited. In the absence of measurement, risk of collision increases with time and employing mission abort algorithms shall be implemented [13]. [14] suggests that the chaser shall keep free drift or hold on points and do not start any new trajectory when the measurements are not available. The constraints on ADR for close approach trajectory due to solar illumination had been briefly discussed in [3] [14] where the chaser shadowing on target had been one of the concerns. However, [3] also underlines that the chaser's Guidance, Navigation and Control (GNC) system is required to be operational with good performance in all illumination conditions since the favourable illumination conditions cannot be guaranteed for ADR targets. Such

unfavourable conditions during the approach are due to the trajectory design which depends on the target attitude profile. [14] suggests that only one fourth of the orbit for Low Earth Orbiting (LEO) ADR targets would have favourable illumination conditions. Considering other constraints on GNC system, it is very much desired to relax the navigation algorithm from illumination conditions point of view.

5 INFRARED IMAGING FACTS

Depending on the temperature, all objects above absolute zero temperature emit electromagnetic radiation in their corresponding spectrum and thermal infrared imagers convert this radiation to image intensity values.

There are two major types of sensing tools for thermal/infrared radiation: thermal detectors and photodetectors. In the case of thermal detectors, responsive elements are sensitive to temperature changes to measure the radiative fluctuations (e.g. bolometers, thermocouples ... etc) whereas photodetectors respond to variations in the number of incident photons (e.g. HgCdTe photodetectors) [15]. Among all, uncooled microbolometers which measure the resistive changes due to thermal radiation are known to be widely used in terrestrial applications since they could provide sufficient sensitivity at low-cost [16]. By considering the cost effectiveness and its promising use in space applications [4] [17], this study focuses on performance of uncooled microbolometer technology.

For infrared imagery, [18] defined four main challenges for working with Infrared images such as "Low SNR-Low Resolution", "Infrared Reflection", "Halo Effect/Saturation" and "History Effects". As it is described "Halo Effect/Saturation" occurs around the objects with high contrast and could be difficult not to associate with the object but this applies to ferroelectric sensors, not microbolometers. The other most important challenge is the "History Effects" which potentially disqualify the use of brightness constancy concept used in optical flow algorithm.

In the context of ADR applications, Infrared imageries also encounter different thermal dynamics compared to their terrestrial counterparts. The targets *Space Debris* change their temperature profile over an orbit (with duration down to 90 minutes) as their geometry with Sun varies over time. Moreover, the man-made materials covering the debris surface also show different response characteristics throughout these quasi-cyclic thermal profiles which makes the thermal scene quite dynamic and unique.

6 INFRARED BASED ADR

In space, thermal environment changes very fast and depends on many parameters which we cannot know perfectly for ADR targets [19]. Even though ADR target exact thermal signature cannot be known, calculations and flown experiments [17][4] suggest that we can observe spacecraft with infrared cameras. However, we have to keep in mind the thermal environment challenges to design a proper navigation system. In our study, we addressed this challenge by assuming the target infrared

appearance model is not available to the navigation algorithm.

Even though the target infrared appearance model is not available, [19] showed that the point features can still be used for target tracking and possibly for recognition purposes. This lead us to a different approach than the earlier model based tracking approaches [20].

Simultaneous Localisation and Mapping (SLAM) is a concept in which the map and the relative position of the observer with respect to this map are estimated at the same time. In relative navigation of chaser for ADR scenario, the map would be infrared features that are detected on the target surface to which chaser would like to know the relative position. We follow the Bayesian filtering approach for the estimation purposes.

The problem had been described by the state vector of $6 + N$ parameters as in Equ-1 with 6 motion parameters $(T_x, T_y, T_z, \omega_z, \omega_x, \omega_y, \omega_z)$ and N structure parameters $(\alpha_w^1, \alpha_w^2, \dots, \alpha_w^N)$ where the global rotation and the 2D points of reference frame (i.e. first frame) has been kept outside the estimation. In order to account the effect of camera focal length on the sensitivity of the image plane motion to camera motion along T_z , the estimation of translation has been performed by $T_z\beta$ parametrisation.

$$x = (T_x, T_y, T_z\beta, \omega_z, \omega_x, \omega_y, \omega_z, \alpha_w^1, \alpha_w^2, \dots, \alpha_w^N) \quad (1)$$

Due to the unexpected dynamics of space debris, the process model has been considered as identity matrix and the inter-frame motion has been modelled with process noise for motion parameters while the landmarks has been kept static as they are part of the space debris rigid body.

7 EXPERIMENTAL WORK

In this section, we present the result of the algorithm for two different data set: synthetic and real infrared imagery where we performed a possible ADR scenario to validate our approach.

Table 1: Camera properties.

Property	Value
Resolution	640x480
HFOV	69°
VFOV	56°
Focal length	9mm
Pixel size	17 μ m

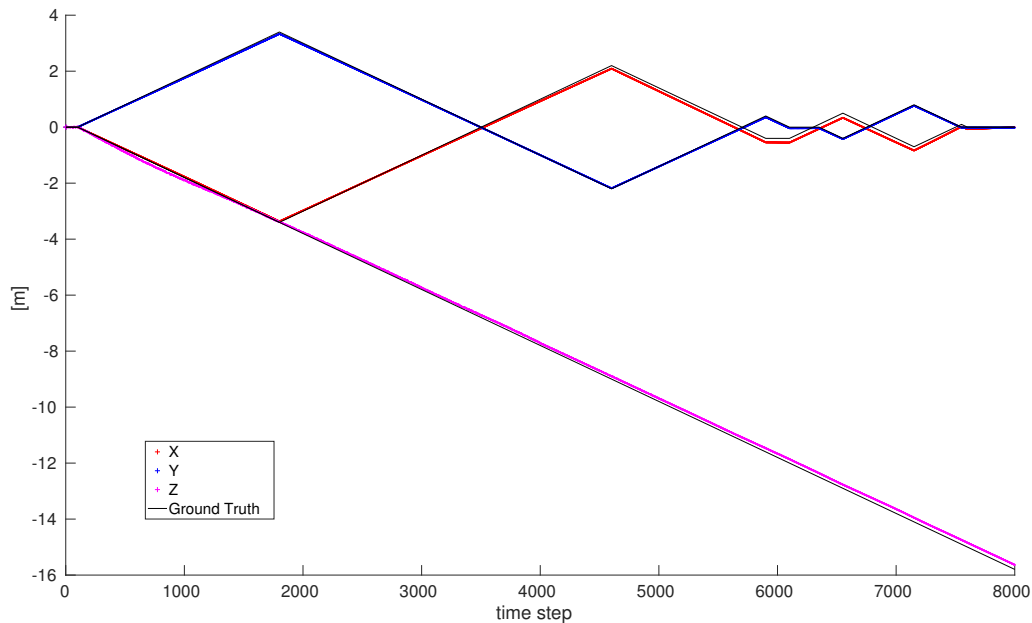


Figure 4: Translational motion of the chaser respect to camera position at first frame

7.1 Synthetic Dataset

This scenario simulates forced translation manoeuvres of the close proximity phase including eight correction manoeuvres which were reflected in 2D projections by sudden changes at the direction of the features' motion fields. In Figure5, only five of these manoeuvres could be observed as we only plotted a limited number of chaser positions for clarity reasons. These manoeuvres would be expected in real scenario due to the close loop control nature of the chaser GNC system. Simulation target range starts from 20 meters and continues until four meter to target.

In order to have a controlled environment in our analysis, we had generated nine synthetic 3D points and then projected them into 2D image points for a camera with properties given in Table-3. To account for the feature tracking errors, the pixel noise $\mathcal{N}(0, \sigma^2)$ had been added into the 2D projection where $\sigma = 0.15\text{pixel}$. In order to be more realistic in our simulations we had also pre-processed the generated 2D points such that features occasionally disappeared from the virtual image for a certain period of time. This modification imitated a quite possible problem of feature tracking algorithms: losing the feature during the tracking. During this process, we had assumed to know the data association between the filter states and the projected features in the virtual frame.

Figure4 and Figure5 show the translational motion of the chaser with respect to world coordinate frame. The ground truth in all axes is represented with the black line. As it would be expected from monocular camera estimations, some error accumulation along the Z-axis had been observed over time. In earlier time steps, one can also observe the small erroneous fluctuations along the Z-axis. This is due to relation between erroneous measurements with their range as the error would be amplified for farther distances due to camera projection geometry.

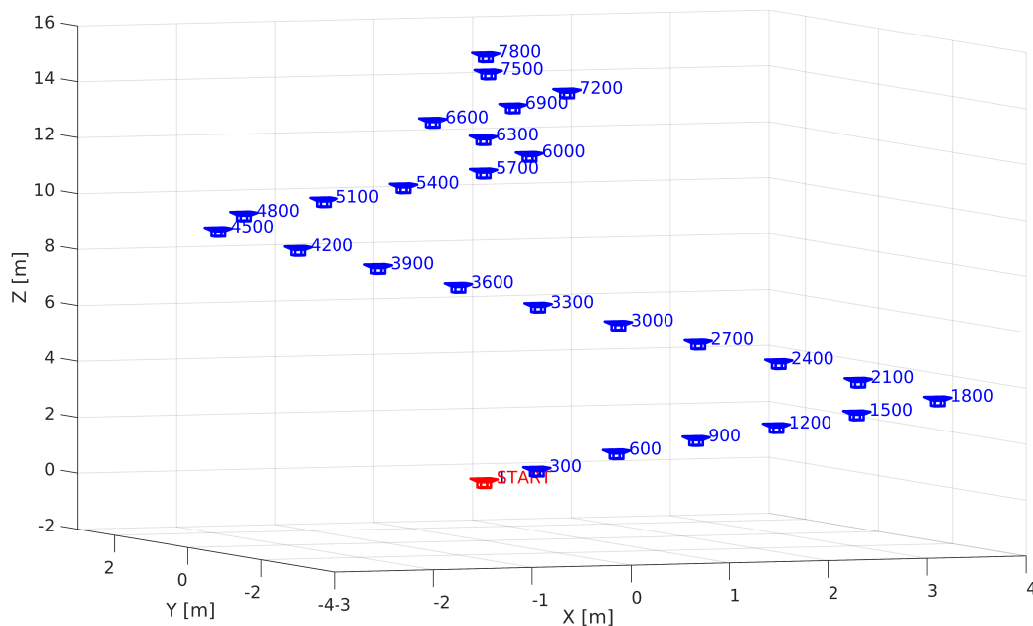


Figure 5: Estimated translational motion of the chaser with respect to camera position at first frame (world frame) in 3D

Between time steps 4000 and 7000, the error along the X-axis had been increased. At the time step 4000, all disappeared features re-appeared again. Therefore, the error along the Y-axis could be linked to the increased uncertainty on those features which were not updated for a while with the relevant measurements. As these features started to disappear from the image, the filter started to be influenced by states which were observed for a longer duration leading to recover the error along the Y-axis.

Figure6 shows the estimation of the feature depths which are represented by different colours and black is the ground truth. At the end of the sequence, all feature depths had error of approximately

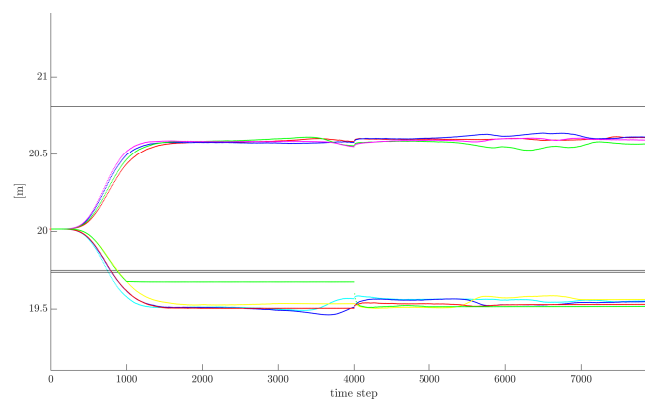


Figure 6: Feature depths with respect to world frame. Each colour represent one feature.

Table 2: Robotic arm properties.

Property	Value
Reach	850mm
Payload	$\leq 5kg$
Repeatability	$\pm 0.1mm$

0.2 meters which is aligned with the error in translational motion estimation along the Z-axis. However, one can clearly see that the ratio between the depths of features were also somehow kept for the estimations. This finding was also expected since the scene can be recovered only up to scale by using monocular camera [21].

7.2 Real Infrared Imagery Dataset

To verify and validate some of the concepts of this research, some experiments have been conducted at the ESTEC GNC Testing Facilities located in Noordwijk, the Netherlands. Our experimental set-up consists of a collaborative robotic arm (Table 2) that is hang on a static robotic arm, thermally representative target placed on a stand, a LWIR camera (Table 3) and a laptop to store our data (Figure 7). Currently the TCP/IP connection of the camera is used at the hardware laboratory of ESTEC to link it with a PC containing the Xenoth Software for camera usage. In order to collect precise positioning of the robotic arm which is holding the camera, we have used the Vicon Motion Capture System (VICON)¹ which consist of seven near infrared cameras and small balls with reflective coating to track the camera and our target. These balls were not affecting our algorithm since our infrared camera is passive however VICON system required very delicate calibration due to optical properties of our target coatings.

Since we had performed our analysis in air, we had achieved the required contrast by heating the target which is a rectangular prism ($192 \times 111 \times 61mm$) (Figure8). The target holds surface coating with different emissivity values which provided sufficient contrast at higher temperatures. We demonstrated the performance of the algorithm for the scaled version of phase-[H] (Figure2) which could typically run for 15-20 minutes. Considering the limitations of the facility such trajectory had been scaled to an experimental run by 1 : 25 which is completed in $\approx 150s$ and every fifth frame was considered as the measurement. As a result, our scaled set-up would correspond to the measurement rate of $\approx 1Hz$ in orbital case.

Figure9 and Figure10 show the translational motion of the chaser with respect to world coordinate frame. The ground truth in all axes is represented with the black line. As it would be expected from

¹<https://www.vicon.com/>

Table 3: Camera properties.

Property	Value
Detector	Uncooled microbolometer
Resolution	384×288
HFOV	29.9°
Focal length	18mm
Aperture	$f/1$
Pixel size	$25\mu\text{m}$
Spectral range	$8\mu\text{m} - 14\mu\text{m}$
Frame rate	23Hz
NETD	$\approx 50\text{mK}$ at 30°C

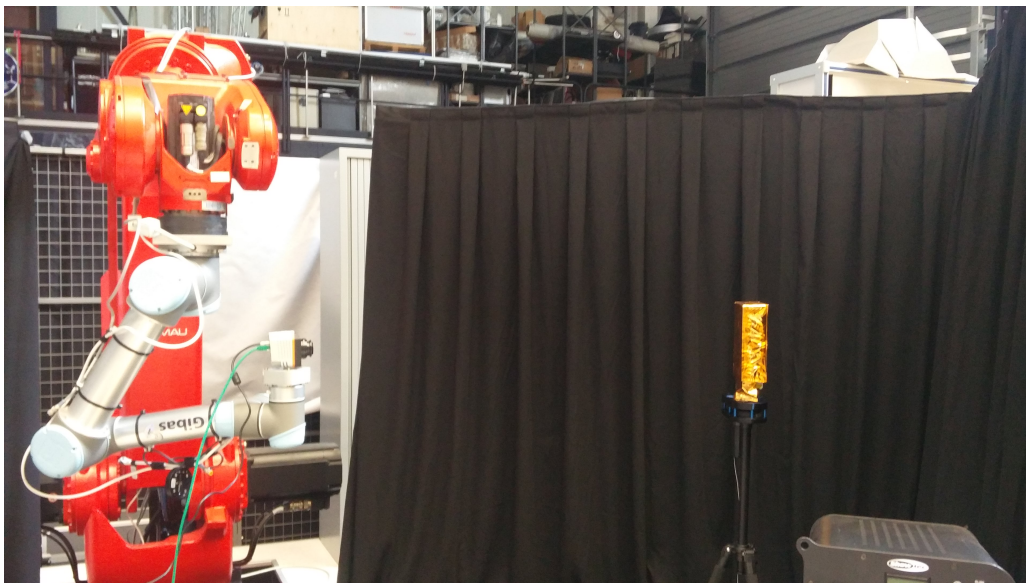


Figure 7: Experimental setup

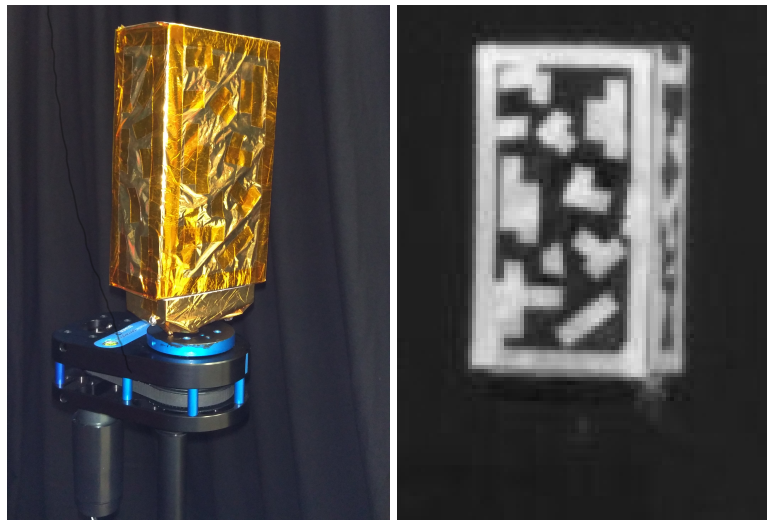


Figure 8: Target in visual (right) and infrared with contrast enhancement of the image acquisition software(left)

monocular camera estimations, some error accumulation along the Z-axis had been observed over time. For camera systems, the accuracy of the system increases as the sensor gets closer to the target therefore the initial estimation errors along X-axis and Y-axis decrease over time.

However, the contribution of the poor resolution and wide pixel size factor of the infrared camera that was used during the experiment ($384 \times 288\text{pixel}$) shall not be forgotten as the error sources. In these kinds of low pixel resolution images the error in image extraction algorithm would have more impact comparing to images of finer detectors. Generally speaking, visual cameras that are used in vision community would most likely have better resolution (e.g. $1024 \times 1024\text{pixel}$ and $6\mu\text{m}$) which would also provide more accurate results. Furthermore, used camera had a very shallow depth of field in which the target was in focus for only certain period of time during the trajectory. Since we had implemented the variations in state parameters as noise which includes focal length, focus adjustment during the course of this experiment would have other complications in the algorithm. To deal with known error sources, we kept the focusing adjustment for 1.1m range which corresponds to last 50s of the trajectory. The performance of feature detection algorithms decreases with the amount of blur. In our case, initial frames are the most blurred ones therefore the measurements are more misleading. Considering that monocular vision cannot resolve the depth information, poor recovery of depth was expected since the estimated depth at the time of focused images would be erroneous.

8 CONCLUSIONS AND FUTURE WORK

The paper showed the review of the state of the art literature in all areas relating to the problem with ADR scenarios, applications, and missions. Then the current ADR proposed missions and the role of Infrared-based navigation for them were explained. The paper explained that the appearance of objects under Sun direct illumination is expected to be smoother in infrared when compared to the reflection of visible light on reflecting surfaces like multi-layer insulation.

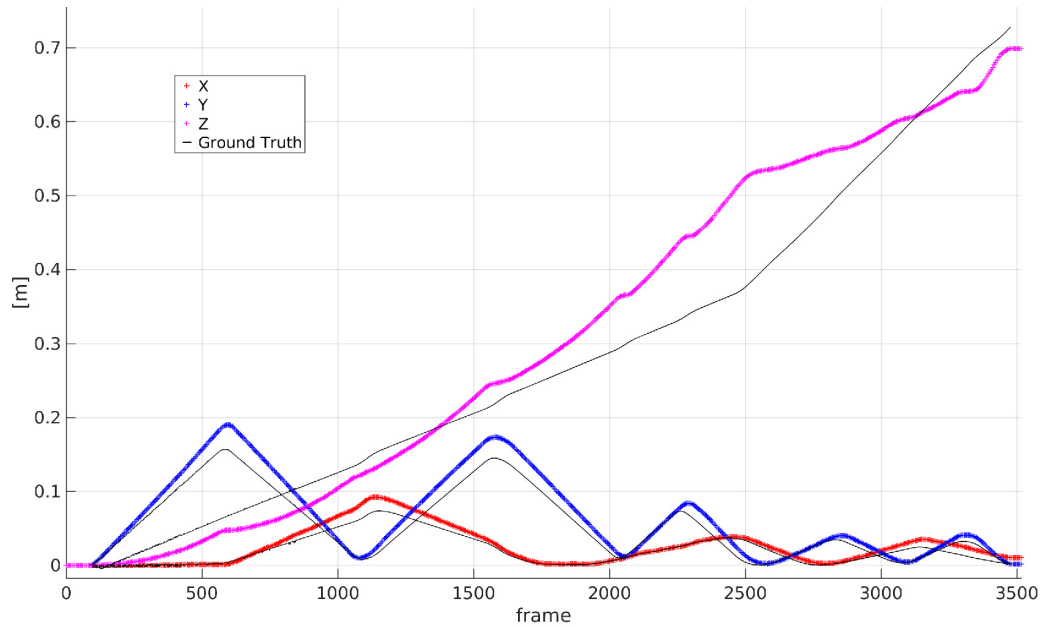


Figure 9: Translational motion of the chaser with respect to camera position at first frame for real infrared imagery

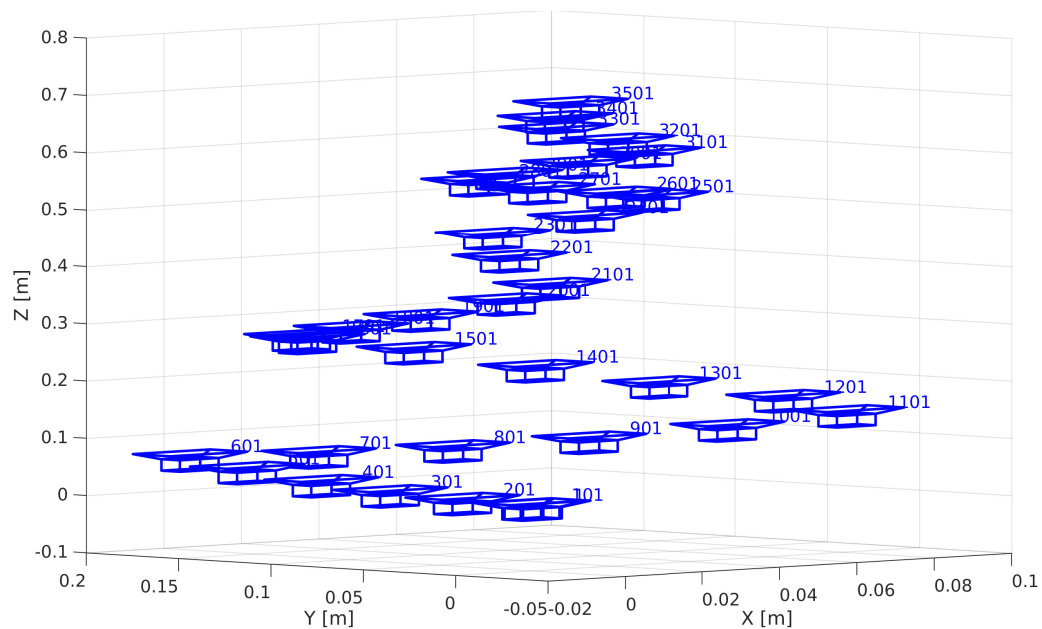


Figure 10: Estimated translational motion of the chaser with respect to camera position at first frame (world frame) in 3D for real infrared imagery

In such cases, thermal imagery has advantages over visual sensors. It can provide continuous information without getting affected by the illumination conditions like eclipse, partial illumination and solar glare. Infrared imagery acquires information about thermal appearance of the target and can provide continuous measurement. This is very beneficial for cases especially like in ADR where there are more unknowns than many different types of rendezvous.

In this study, we have seen that infrared imagery could provide sufficient information for relative navigation purposes in ADR. However, it is very important to have more real space imagery data especially from real space debris to verify developed algorithms. LIRIS experimental data shall be analysed with care as the subject of interest is not actually a space debris and may have more optimistic conditions. We have also shown that the SLAM based approach are suitable for infrared imagery where the target appearance model cannot be provided due several reasons. Therefore, it is considered to be more tolerant to the unknowns of ADR and infrared based ADR. The initialisation of this approach would be faster and computationally less heavy than model based approaches since it will use all available data.

The current state of the algorithm being developed can perform for relative translational motions between chaser and target for a rotationally static target with any relative orientation with respect to the chaser. As future work, the approach will be developed further for the cases where the target is tumbling in order to encapsulate wider range of target attitude .

9 ACKNOWLEDGEMENT

The study has been funded and supported by European Space Agency and Sodern under Network Partnership Initiative program with grant number NPI 342-2014.

Authors would like to thank Shubham Vyas and Jan Smissek for their support during the experimental set-up.

REFERENCES

- [1] C. Bonnal, J.-M. M. Ruault, and M.-C. C. Desjean, "Active debris removal: Recent progress and current trends," *Acta Astronautica*, vol. 85, pp. 51–60, apr 2013. [Online]. Available: <http://www.sciencedirect.com/science/article/pii/S0094576512004602>
- [2] K. Wormnes, R. L. Letty, L. Summerer, R. Schonenborg, E. Luraschi, A. Cropp, H. Krag, and J. Delaval, "ESA Technologies For Space Debris Remediation," in *Proceedings of the 6th IAASS Conference: Safety is Not an Option*, 2006.
- [3] J. A. F. Deloo and E. Mooij, "Active debris removal : Aspects of trajectories , communication and illumination during final approach," *Acta Astronautica*, vol. 117, pp. 277–295, 2015. [Online]. Available: <http://dx.doi.org/10.1016/j.actaastro.2015.08.001>

- [4] B. Cavrois, A. Vergnol, A. Donnard, P. Casiez, U. Southivong, O. Mongrard, F. Ankersen, C. Pezant, P. Bretecher, F. Kolb, and M. Windmuller, “LIRIS demonstrator on ATV5 : a step beyond for European non cooperative navigation system,” in *AIAA Guidance, Navigation, and Control Conference*, 2015.
- [5] L. Infrared, “Space In Images,” 2014. [Online]. Available: http://www.esa.int/spaceinimages/Images/2014/12/LIRIS{_}infrared
- [6] D. Kucharski, G. Kirchner, F. Koidl, C. Fan, R. Carman, C. Moore, A. Dmytrotso, M. Ploner, G. Bianco, M. Medvedskij, A. Makeyev, G. Appleby, M. Suzuki, J. M. Torre, Z. Zhongping, L. Grunwaldt, and Q. Feng, “Attitude and spin period of space debris envisat measured by satellite laser ranging,” *IEEE Transactions on Geoscience and Remote Sensing*, vol. 52, no. 12, pp. 7651–7657, 2014.
- [7] S.-i. Nishida, S. Kawamoto, Y. Okawa, F. Terui, and S. Kitamura, “Space debris removal system using a small satellite,” *Acta Astronautica*, vol. 65, pp. 95–102, 2009.
- [8] W. Fehse, *Automated Rendezvous and Docking of Spacecraft*, 1st ed. Cambridge: Cambridge University Press, 2003.
- [9] S. Nakasuka and T. Fujiwara, “New method of capturing tumbling object in space and its control aspects,” in *IEEE International Conference on Control Applications*, no. 1, 1999.
- [10] S.-i. Nishida and S. Kawamoto, “Strategy for capturing of a tumbling space debris,” *Acta Astronautica*, vol. 68, no. 1-2, pp. 113–120, 2011. [Online]. Available: <http://dx.doi.org/10.1016/j.actaastro.2010.06.045>
- [11] F. Terui, H. Kamimura, and S. ichiro Nishida, “Motion Estimation to a Failed Satellite on Orbit using Stereo Vision and 3D Model Matching,” in *9th International Conference on Control, Automation, Robotics and Vision*, 2006, pp. 1–8.
- [12] N. W. Oumer, G. Panin, Q. Mülbauer, and A. Tseneklidou, “Vision-based localization for on-orbit servicing of a partially cooperative satellite,” *Acta Astronautica*, vol. 117, pp. 19–37, 2015. [Online]. Available: <http://linkinghub.elsevier.com/retrieve/pii/S0094576515003069>
- [13] G. M. Hoffmann, D. Gorinevsky, R. W. Mah, C. J. Tomlin, and J. D. Mitchell, “Fault Tolerant Relative Navigation using Inertial and Relative Sensors,” in *AIAA Guidance, Navigation and Control Conference and Exhibit*, no. August, 2007, pp. 1–18.
- [14] W. Fehse, “Rendezvous With and Capture / Removal of Non-cooperative Bodies in Orbit The Technical Challenges,” *Journal of Space Safety Engineering*, vol. 1, no. 1, pp. 17 – 27, 2014.
- [15] W. L. Wolfe, “Detectors,” in *Handb. Mil. Infrared Technol.*, 1965, pp. 458–519.
- [16] L. J. Kozlowski and W. F. Kosonocky, “Infrared Detector Arrays,” in *Handbook of Optics Volume 2*, 1995, ch. 33. [Online]. Available: http://www.mhprofessional.com/handbookofoptics/pdf/Handbook{_}of{_}Optics{_}vol2{_}ch33.pdf

- [17] S. Ruel, T. Luu, and A. Berube, “Space shuttle testing of the TriDAR 3D rendezvous and docking sensor,” *Journal of Field Robotics*, pp. 535–553, 2012.
- [18] K. Hajebi and J. S. Zelek, “Structure from Infrared Stereo Images,” *2008 Canadian Conference on Computer and Robot Vision*, pp. 105–112, 2008. [Online]. Available: <http://ieeexplore.ieee.org/lpdocs/epic03/wrapper.htm?arnumber=4562100>
- [19] O. Yilmaz, N. Aouf, L. Majewski, and M. Sanchez-Gestido, “Evaluation of Feature Detectors for Infrared Imaging In View of Active Debris Removal,” in *7th European Conference on Space Debris*, 2017.
- [20] A. Petit, E. Marchand, and K. Kanani, “Tracking complex targets for space rendezvous and debris removal applications,” in *Intelligent Robots and Systems (IROS)*, 2012.
- [21] R. Hartley and A. Zisserman, *Multiple View Geometry in Computer Vision*, 2nd ed., 2004.